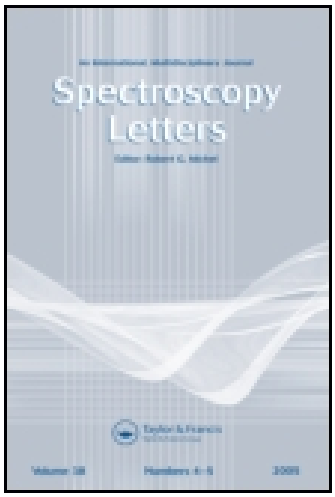

Spectroscopy Letters: An International Journal for Rapid Communication

Publication details, including instructions for authors and subscription information:
http://www.tandfonline.com/loi/lstl20

Metal-Based Molecular Design Tuning Biochemical Behavior: Synthesis, Characterization, and Biochemical Studies of Mixed Ligand Complexes Derived From 4-Aminoantipyrine Derivatives

J. Joseph [a] & G. Ayisha Bibin Rani [a]

[a] Department of Chemistry , Noorul Islam Centre for Higher Education , Kumaracoil , Tamilnadu , India

Accepted author version posted online: 05 Mar 2013.Published online: 03 Dec 2013.

To cite this article: J. Joseph & G. Ayisha Bibin Rani (2014) Metal-Based Molecular Design Tuning Biochemical Behavior: Synthesis, Characterization, and Biochemical Studies of Mixed Ligand Complexes Derived From 4-Aminoantipyrine Derivatives, Spectroscopy Letters: An International Journal for Rapid Communication, 47:2, 86-100, DOI: 10.1080/00387010.2013.776087

To link to this article: http://dx.doi.org/10.1080/00387010.2013.776087

Spectroscopy Letters, 47:86–100, 2014

ISSN: 0038-7010 print/1532-2289 online
DOI: 10.1080/00387010.2013.776087

Taylor & Francis
Taylor & Francis Group

Metal-Based Molecular Design Tuning Biochemical Behavior: Synthesis, Characterization, and Biochemical Studies of Mixed Ligand Complexes Derived From 4-Aminoantipyrine Derivatives

J. Joseph
and G. Ayisha Bibin Rani

Department of Chemistry, Noorul Islam Centre for Higher Education, Kumaracoil, Tamilnadu, India

ABSTRACT Biosensitive mixed ligand complexes of metals (Fe(III), Co(II), Ni(II), Cu(II), and Zn(II)) with the Schiff bases of L^1 and HL^2 (L^1: obtained through the condensation of 4-aminoantipyrine with furfuraldehyde; HL^2: derived from 2-aminophenol and 3-nitrobenzaldehyde) were synthesized. They were characterized using elemental analysis, magnetic susceptibility, molar conductance, proton nuclear magnetic resonance spectroscopy, ultraviolet–visible spectroscopy, infrared, and electron spin resonance techniques. Cyclic voltammogram of the complexes in dimethylsulfoxide solution at 300 K was recorded and their salient features were summarized. The X-band electron spin resonance spectrum of the copper complex in dimethylsulfoxide solution at 300 and 77 K was recorded. The in vitro biological screening effects of the investigated compounds were tested against the bacterial species *Staphylococcus aureus, Escherichia coli, Klebsiella pneumoniae, Proteus vulgaris,* and *Pseudomonas aeruginosa* and the fungal species *Aspergillus niger, Rhizopus stolonifer, Aspergillus flavus, Rhizoctonia bataicola,* and *Candida albicans* by disc diffusion method. Comparative study of inhibition values of the Schiff bases and their complexes indicates that the complexes exhibit higher antimicrobial activity than the free ligands. DNA binding studies of metal complexes using ultra-violet-visible spectroscopy and cyclic voltammetry paved the way to probe their DNA binding abilities. The solvatochromism and superoxide dismutase activity of these complexes have also been examined.

KEYWORDS 4-aminoantipyrine, disc diffusion, DNA binding, mixed ligand metal complexes, SOD

Received 14 January 2013; accepted 11 February 2013.

Address correspondence to J. Joseph, Department of Chemistry, Noorul Islam Centre for Higher Education, Kumaracoil-629180, Tamilnadu, India. E-mail: chem_joseph@yahoo.co.in

INTRODUCTION

Transition metal complexes with oxygen and nitrogen donor ligands are of great interest for their ability to possess unusual configurations, their structural lability, and their sensitivity to molecular environments.[1] Ternary complexes formed between metal ions and two different types of bioligands, namely, heteroaromatic nitrogen bases and Schiff bases, may be considered as models for substrate metal ion–enzyme interactions and other metal ion–mediated biochemical interactions.[2] Antipyrine (AP) was first synthesized by Knorr in 1883, and there has been a continued interest in the studies of antipyrine derivatives (APDs). APDs have been accepted as important biomodel compounds in the biological systems, and research works have been carrying on with new compound findings. In the coordination chemistry, APDs were extensively used as a group of important ligands due to the coordinated function of the keto or aza-groups.[3] APDs have exhibited attractive multifunctional properties as coordinate, antioxidant, antiputrefactive, and optical characteristics in chemical and material fields.[4] Schiff bases of 4-aminoantipyrine and its complexes are known for their variety of applications in the area of catalysis, clinical applications, and pharmacology. New kinds of chemotherapeutic agents containing Schiff bases have gained significant attention among biochemists, and of those aminopyrines are commonly administered intravenously to detect liver disease in clinical treatment.[5] Schiff bases are potential anticancer drugs and, when administered as their metal complexes, the anticancer activity of these complexes is enhanced in comparison to the free ligand. Schiff bases of 4-aminoantipyrine and its complexes present a great variety of biological activities, including antitumor, fungicide, bactericide, antiinflammatory, and antiviral activities.[6] Aminophenols are also important to the pharmaceutical industry, since they have antibacterial and antitubercular action. Schiff bases obtained from the condensation of 2-aminophenol with some aldehydes and ketones have also been used widely as antituberculosis compounds, and their importance is mainly due to their ability to form metal chelates.[7]

To discover new therapeutic agents that specifically target DNA, it is essential to understand the action mechanism of some DNA-targeted drugs and toxic agents as well as the origins of some diseases like gene mutation. Many compounds expose their antitumor activity through binding to DNA and can cause DNA damage in cancer cells by blocking the division of cancer cells and resulting in cell death.

Superoxide dismutase activity (SOD) in conjunction with catalase appears to be the most effective enzymatic defense against the toxicity of oxygen metabolism. Among the known SOD enzymes, CuZn(SOD) is the most efficient catalytic species. It catalyzed the disproportionation of the cytotoxic superoxide radical $O_2^{\bullet -}$, to oxygen and hydrogen peroxide, through one electron redox cycle involving its copper center. It has been known since three decades ago that cancer cells have less than normal SOD activity and treatment with bovine-native CuZn-SOD decreased the growth of several solid tumors.[8]

The superoxide radical anion $O_2^{\bullet -}$ is formed as a byproduct of normal cellular respiration. Its decomposition produces undesired harmful species like hydroxyl radical and hydrogen peroxide. To control this, nature has created a family of enzymes that remove them from the cellular environment. One of these, SOD, catalyzes the disproportionation of superoxide to dioxygen and hydrogen peroxide, which is decomposed via being catalyzed to water and dioxygen.[9]

Inspired from the literature facts, the present study focused on the mixed ligand transition metal complexes of Schiff bases of L^1 and HL^2 toward tuning of biochemical potentials. They were characterized using analytical and spectral techniques. The biochemical studies of complexes were also performed.

MATERIALS AND METHODS

Materials

All chemicals used in the present work, viz., 4-aminoantipyrine, furfuraldehyde, 2-aminophenol, 3-nitrobenzaldehyde, Fe(III), Co(II), Ni(II), Cu(II), and Zn(II) chlorides, were of analytical reagent grade (Merck, Darmstadt, Germany). The solvents used were distilled before use. Calf thymus DNA was purchased from Genie Biolab (Bangalore, India).

Instrumentation

The elemental analysis was performed using a PerkinElmer 2400 CHN elemental analyzer (PerkinElmer, Waltham, Massachusetts, USA). IR spectra of

the Schiff base ligands and their metal complexes were recorded on a PerkinElmer FT-IR 783 spectrophotometer (PerkinElmer, Waltham, Massachusetts, USA) in the 4000–300 cm^{-1} range using KBr disc. ^{1}H-NMR spectra were recorded on a Bruker Avance Dry 300 MHz FT-NMR spectrometer (Bruker, Rheinstetten, Germany) in dimethylsulfoxide (DMSO) with tetramethylsilane (TMS) as the internal reference. The FAB mass spectrum of the Schiff base ligands and their complexes were recorded on a JEOL S × 102/DA-6000 mass spectrometer/data system (JEOL, Vernon Hills, Illinois, USA) using argon/xenon (6 kV, 10 mA) as the FAB gas. The electron paramagnetic resonance spectrum of the mixed ligand copper complex was recorded on a Varian E 112 EPR spectrometer (JEOL, Japan) in DMSO solution both at room temperature (300 K) and at liquid nitrogen temperature (77 K) using TCNE (tetracyanoethylene) as the g marker. Electronic absorption spectra were recorded in DMSO using a Systronics 2201 double-beam UV-Vis spectrophotometer (Systronics, Ahmedabad, India). Molar conductance of the copper complexes was measured in DMSO solution using a Coronation digital conductivity meter (Coronation, Ahmedabad, India). The magnetic susceptibility values were calculated using the relation $\mu_{eff} = 2.83(\chi_m .T)^{1/2}$ BM. The diamagnetic corrections were made by Pascal's constant and $Hg[Co(SCN)_4]$ was used as a calibrant. The amount of metal present in the metal complexes was estimated using the ammonium oxalate method. Electrochemical experiments were performed on a CHI 604D electrochemical analysis system (CH Instruments, Inc., Austin, Texas, USA) with a three-electrode system consisting of a glassy carbon working electrode, Pt wire auxiliary electrode, and Ag/AgCl reference electrode. Tetrabutylammoniumperchlorate (TBAP) was used as the supporting electrolyte. All solutions were purged with N_2 for 30 min prior to each set of experiments. Calf thymus DNA was purchased from Genie Biolab (Bangalore, India). Tris–HCl buffer solution used for binding studies was prepared using deionized double-distilled water.

Preparation

Preparation of Ligands

L^1: The ligand (L^1) was prepared as reported previously.[10]

The Schiff base FAAP was prepared by a dropwise addition, with stirring, of ethanolic solution (20 cm^3) of furan-2-carboxaldehyde (1.0 g, 0.01 M) to an ethanolic solution (25 cm^3) of 4-aminoantipyrine (2.1 g, 0.01 M), respectively. The reaction mixture was refluxed on a water bath for 1–2 hr. On cooling, the solid products were separated and filtered. Both Schiff physical measurement bases were recrystallized from ethanol and dried in vacuo over P_4O_{10}, to yield yellow crystals.

HL^2: The ligand (HL^2) was prepared as reported previously.[11]

The Schiff base was synthesized by stirring a mixture of 3-nitro benzaldehyde (1.51 g, 0.01 M) with 2-aminophenol (1.09, 0.01 M) in 50 mL of ethanolic medium. The solid product formed was removed by filtration and recrystallized from ethanol.

Preparation of Metal Complexes

An ethanolic solution of metal (II) (M=$FeCl_3.6H_2O$, $CoCl_2.6H_2O$, $NiCl_2.6H_2O$, $CuCl_2.2H_2O$ & $ZnCl_2$) (1 mM) was stirred with an ethanolic solution of ligands (L^1 and HL^2) (1 mM) and the resultant mixture was refluxed for ca. 6–8 hr. Then the volume of solution was reduced to one-third on a water bath. The solid complex precipitated was filtered, washed thoroughly with ethanol, and dried in vacuum.

The schematic route for synthesis of Schiff base ligands and their metal complexes is given in Scheme 1.

DNA-Binding Assay

Interaction of the complex with calf thymus DNA has been studied by recording electronic absorption spectra. A solution of CT-DNA in 5 mM Tris–HCl/50 mM NaCl (pH 7.0) gave a ratio of UV absorbance at 260 and 280 nm (A_{260}/A_{280}) of 1.8–1.9, indicating that the DNA was sufficiently free of proteins. A concentrated stock solution of DNA was prepared in 5 mM Tris–HCl/50 mM NaCl in water at pH 7.0 and the concentration of CT-DNA was determined per nucleotide by taking the absorption coefficient (6600 $dm^3\ mol^{-1}\ cm^{-1}$) at 260 nm. Doubly distilled water was used to prepare buffer solutions. Solutions were prepared by mixing the complex and CT-DNA in DMF medium. After equilibrium was reached (ca. 5 min) the spectra were recorded against an analogous blank solution containing the

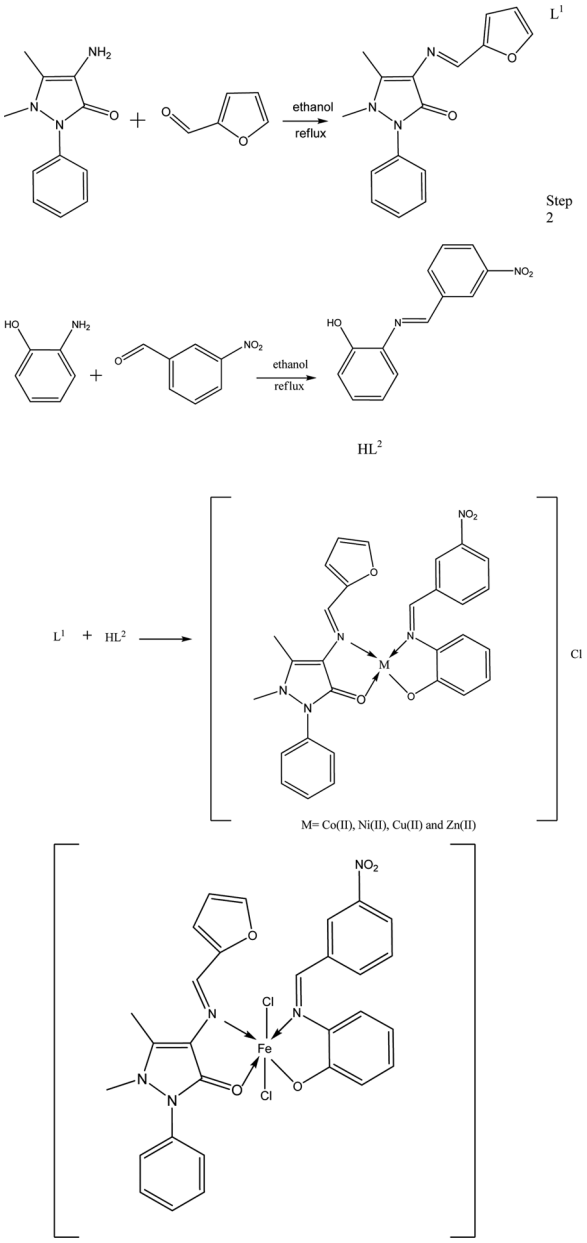

SCHEME 1 **Schematic route for synthesis of schiff base ligands and their metal complexes.**

same concentration of DNA. UV spectral data were fitted into Eq. (1) to obtain the intrinsic binding constant (K_b).

$$[DNA]/(\varepsilon_a - \varepsilon_f) = [DNA]/(\varepsilon_b - \varepsilon_f) + K_b(\varepsilon_b - \varepsilon_f) \quad (1)$$

where [DNA] is the concentration of DNA in base pairs; ϵ_a, ϵ_b, and ϵ_f are apparent extinction coefficients (A_{obs}/[M]), the extinction coefficient for the metal (M) complex in the fully bound form and the extinction coefficient for free metal (M), respectively. A plot of [DNA]/($\epsilon_a - \epsilon_f$) versus [DNA] gave a slope of 1/($\epsilon_b - \epsilon_f$) and Y-intercept equal to 1/K_b($\epsilon_b - \epsilon_f$); K_b is the ratio of the intercept.

Antimicrobial Activity

The in vitro evaluation of antimicrobial activity was carried out. The synthesized compounds were tested against some fungi and bacteria to provide the minimum inhibitory concentration (MIC) for each compound. The MIC is the lowest concentration of solution to inhibit the growth of a test organism. The in vitro biological screening effects of the investigated compounds were tested against the bacterial species and fungal species by the disc diffusion method. One day prior to the experiment, the bacterial and fungal cultures were inoculated in nutrient broth (inoculation medium) and incubated overnight at 37°C. Inoculation medium containing 24-hr-grown culture was added aseptically to the nutrient medium and mixed thoroughly to get uniform distribution. This solution was poured (25 mL in each dish) into Petri dishes and then allowed to attain room temperature. Wells (6 mm in diameter) were cut in the agar plates using proper sterile tubes. Then, the wells were filled up to the surface of agar with 0.1 mL of the test compounds dissolved in DMSO (200 μg/mL). The plates were allowed to stand for an hour to facilitate the diffusion of the drug solution. Then the plates were incubated at 37°C for 24 hr for bacteria and 48 hr for fungi and the diameter of the inhibition zones was measured. MICs were detected by the serial dilution method. The lowest concentration (μg/mL) of compound, which inhibits the growth of bacteria after 24-hr incubation at 37°C and of fungi after 72-hr incubation at 37°C, was taken as the MIC.

Superoxide Dismutase (SOD) Activity

In vitro SOD activity was measured using alkaline DMSO as a source of superoxide radical ion ($O_2^{\cdot-}$) and nitrobluetetrazolium (NBT) as $O_2^{\cdot-}$ scavenger.[12] In general, 400 μL of the sample to be assayed was added to a solution containing 2.1 mL of 0.2 M potassium phosphate buffer (pH 7.8) and 1 mL of 56 μM NBT. The tubes were kept in ice for 20 min and then 1.5 mL of alkaline DMSO solution was added while stirring. The absorbance was then monitored at 540 nm against a sample prepared under

similar conditions except that NaOH was absent in DMSO. The percentage inhibition (η) of NBT reduction was calculated using the following equation:

$$(\%\ \text{Inhibition of NBT reduction}) = (1 - k'/k) \times 100$$

where, k′ and k represent the slopes of the straight line of absorbance values as a function of time in the presence and in the absence of SOD mimic or a model compound, respectively. The IC_{50} value of the complex was determined by plotting the graph of percentage inhibition of NBT reduction against an increase in the concentration of complex. The concentration of the complex that causes 50% inhibition of NBT reduction is reported as IC_{50}.

RESULTS AND DISCUSSION

The Schiff base ligands and their mixed ligand complexes have been synthesized and characterized by spectral and analytical techniques. The color, analytical data, molar conductance, and magnetic moment values are given in Table 1. The elemental analyses of the Schiff base ligands support the chemical composition of the ligands and their complexes. In the present study, the prepared complexes are 1:1 electrolytic in nature, except the iron complex (nonelectrolytic in nature). All the complexes are stable in air. The antipyrine derivatives are found to be soluble in chloroform, dimethylformide, tetrahydrofuran, and dimethylsulphoxide.

^{1}H-NMR Spectra

The ligand (L^1) shows the following signals and their assignments are given below: phenyl multiplet at 7.3–7.5 δ (5H), -CH=N at 7.9 (due to furfuryl moiety), -C-CH_3 at 2.4 δ, N-CH_3 at 3.2 δ. The ligand (HL^2) shows that the following signals are assigned as phenyl multiplet at 7.1–7.9 δ (8H), -CH=N at 8.5 δ (due to phenyl moiety), and -OH at 10.4 ppm (s, 1H). The azomethine proton (-CH=N) signal in the spectrum of zinc (II) complex is shifted downfield compared to the free ligands, suggesting deshielding of the azomethine group due to the coordination with metal ions. The phenolic OH proton in the ligand (HL^2) disappeared in the zinc (II) complex, suggesting that the -OH proton is involved in coordination.[11] The ^{1}H-NMR spectrum of the zinc (II) complex is shown in Fig 1.

IR Spectra

To study the binding mode of the Schiff base to the metal complexes, the IR spectra of the free ligands were compared with the spectra of the complexes. The absorption band at 1647 cm^{-1} is assigned ν(C=O) in L^1 free ligand. The shift of bands to lower wavenumber 20–32 cm^{-1} in the spectra of all complexes suggests the involvement of the pyrazolone oxygen in chelation. The strong absorption bands located at 1616 and 1603 cm^{-1} in the spectrum of the free ligands L^1 and HL^2 are attributed to ν(-CH=N) vibrations. These bands are shifted (by $\sim$10–40 cm^{-1}) toward lower frequencies in the spectra of all the complexes, which clearly indicated that the complexation has taken place through the nitrogen atom of the azomethine group.

The IR spectra of the ligands show a strong band in the 3050–3400 cm^{-1} region, assigned to the phenolic -OH group. The disappearance of this band in the spectra of the complexes indicates the deprotonation of the hydroxyl group upon coordination. The IR spectra of the metal complexes also show some new bands in the 480–450-cm^{-1} and 447–410-cm^{-1} regions, which may probably be due

TABLE 1 Physical and Analytical Data of the Synthesized Complexes

Compound	Color	Yield %	Elemental analysis				Molar conductance (Ω^{-1} cm^2 mol^{-1})	μ_{eff} (BM)
			C	H	N	M		
L^1	Yellow	85%	68.30 (68.2)	5.38 (5.37)	14.94 (14.92)	—	—	—
HL^2	Yellow	81%	64.44 (64.41)	4.16 (4.12)	11.57 (11.60)	—	—	—
$[FeL^1L^2\ Cl_2]$	Brown	80%	50.77 (50.75)	3.68 (3.65)	10.22 (10.25)	8.15 (8.12)	6	5.6
$[CoL^1L^2]$ Cl	Brown	82%	53.29 (53.28)	3.86 (3.81)	10.72 (10.75)	9.02 (9.05)	38	3.12
$[NiL^1L^2]$ Cl	Brown	78%	53.31 (53.34)	3.86 (3.85)	10.73 (10.70)	8.99 (8.96)	54	Dia
$[CuL^1\ L^2]$Cl	Brown	82%	52.92 (52.90)	3.83 (3.80)	10.65 (10.63)	9.66 (9.65)	45	1.81
$[ZnL^1L^2]$ Cl	Dark Yellow	84%	52.77 (52.72)	3.82 (3.85)	10.62 (10.60)	9.92 (9.95)	38	Dia

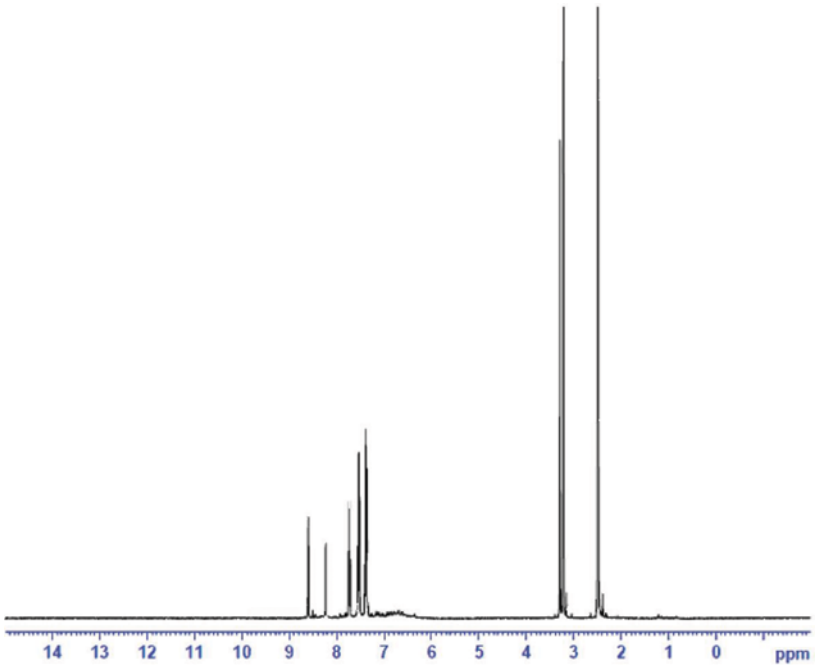

FIGURE 1 ^{1}H-NMR spectrum of zinc (II) complex. (Color figure available online.)

to the formation of ν(M-O) and ν(M-N) bands, respectively. In the case of the Fe(III) complex, the weak band that appeared at 350 cm^{-1} is due to the formation of Fe–Cl bond. IR spectral data of the ligands (L^1 [Fig. 2a] and HL^2 [Fig. 2b]) and copper complex (Fig. 2c) are presented in Table 2.

Electronic Absorption Spectra

The electronic absorption spectral data of the ligands and their complexes were recorded in DMSO and are presented in Table 3. The electronic spectrum of free Schiff base ligand show bands at 31,300 (320 nm) and 30,581 cm^{-1}(327 nm), which is assigned to the π-π^* transitions of the azomethine (>C=N–) chromophore. On complexation this band was shifted to lower wavelengths, suggesting the coordination of azomethine nitrogen to the central metal ion.

The electronic spectrum of the Fe(III) complex exhibits bands at 19,064 (525 nm) and 20,265 cm^{-1} (494 nm) and are attributable to $^{6}A_{1g}\rightarrow{}^{4}T_{1g}$(G) and $^{6}A_{1g}\rightarrow{}^{4}T_{1g}$(G) transitions, respectively. In these transitions two intense bands may be assigned spin-forbidden d–d transitions and the other charge-transfer transitions. These transitions are assigned for octahedral Fe(III) complexes. The electronic transitions together with the magnetic moment value of 5.6 BM suggested high-spin octahedral geometry for the Fe(III) complex.[13]

The spectrum for the Co(II) complex shows a d–d band at 18,651 (537 nm) and 31,532 cm^{-1} (317 nm) and may be assigned to $^{1}A_{1g}\rightarrow{}^{1}B_{g}$, respectively, in square planar stereochemistry. Together with the magnetic moment value of 3.12 BM, a square planar geometry for the Co(II) complex was proposed.

The electronic spectrum of the nickel (II) complex shows two d–d bands at 20,126 (497 nm) and 18,670 cm^{-1}(536 nm), which are assigned as $^{1}A_{1g}\rightarrow{}^{1}B_{1g}$ and $^{1}A_{1g}\rightarrow{}^{1}B_{2g}$ transitions, indicating the square planar geometry.[14] This complex is diamagnetic in nature. Therefore, a square planar geometry has been suggested.

In the present study, the copper (II) complex exhibits bands at 18,302 cm^{-1}(546 nm) and 20,823 cm^{-1} (480 nm) assigned to $^{2}B_{1g}\rightarrow{}^{2}A_{1g}$ transitions characteristic of a square planar geometry with $d_{x^2-y^2}$ ground state.[15–17] These data and the magnetic moment value of 1.81 BM suggest square planar geometry around Cu(II).

In general, Zn(II) is a d^{10} metal ion; no band is expected in the visible region and it is also found as a diamagnetic complex. However, a strong band observed at 22,172 cm^{-1} (451 nm) is assignable to the L→M charge transfer transition,[18] which is compatible with this complex having a square planar geometry.

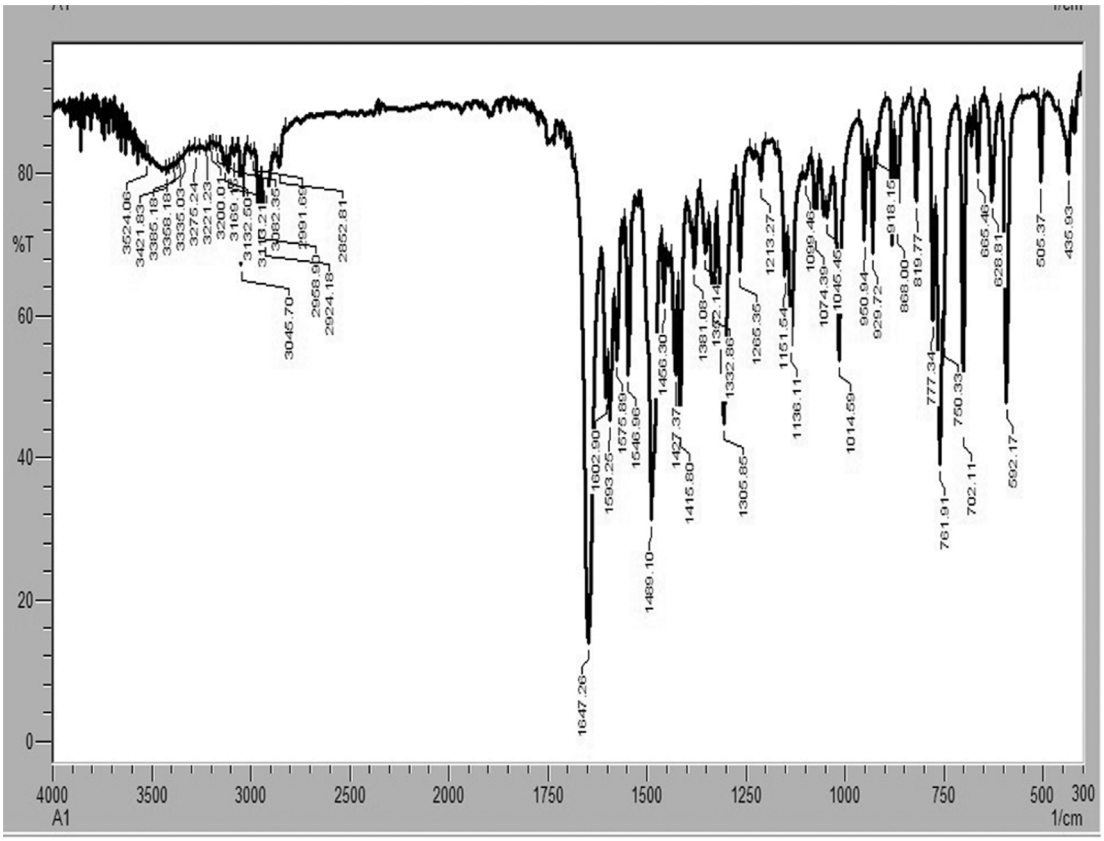

(a)

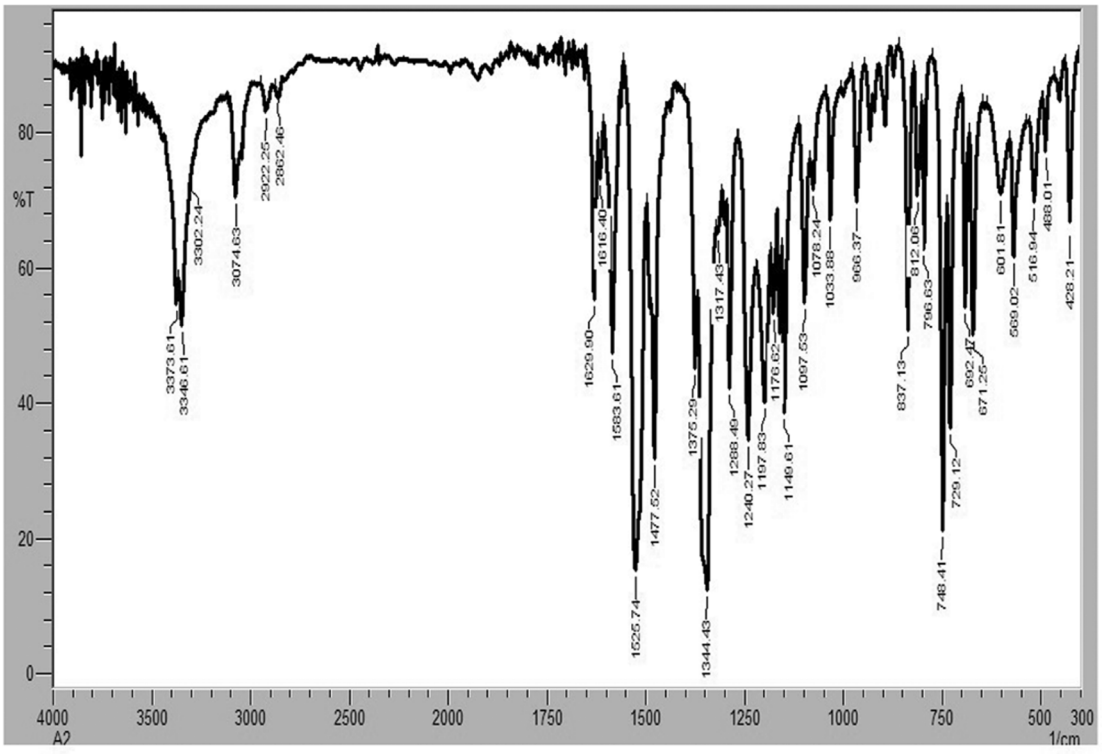

(b)

FIGURE 2 **IR spectrum of ligands (L^1(2) and HL^2 (b)) and copper complex (c).**

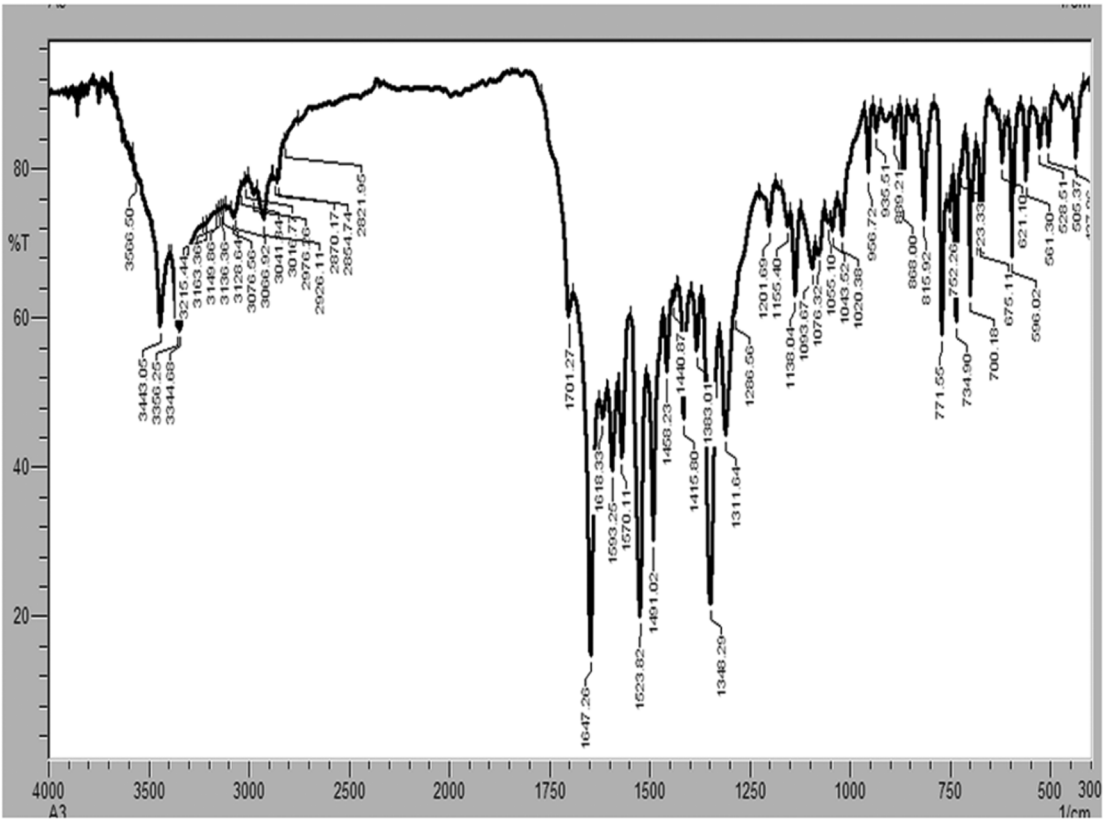

(c)

FIGURE 2 CONTINUED.

ESR Spectra

The ESR spectrum of the copper complex was recorded in DMSO at 300 and 77 K (Fig. 3). The observed trend of $g\|(2.21) > g_{\perp}(2.02) > g_e(2.0023)$ describes the axial symmetry with the unpaired electron residing in the d_{x2-y2} orbital.[19] The value of $g_{\|} < 2.2$ in the present copper complex gives a clear indication of the covalent character of the metal–ligand bond and delocalization of the unpaired electron into the ligand.

TABLE 2 **IR Spectral Data (cm^{-1}) for the Free Ligands and Their Metal Complexes**

Compound	ν C=O	ν C=N	ν M-O	ν M-N	ν M-Cl
L^1	1647	1616	—	—	—
HL^2	—	1603	—	—	—
$[FeL^1L^2Cl_2]$	1637	1579 1584	471	434	350
$[CoL^1L^2]$ Cl	1641	1575 1576	453	429	—
$[NiL^1L^2]$ Cl	1632	1596 1593	480	434	—
$[CuL^1L^2]$Cl	1643	1583 1578	450	410	—
$[ZnL^1L^2]$ Cl	1639	1591 1589	478	447	—

The EPR parameters $g_{\|}$, $g_{\perp}$, and $A_{\|}$ and the energies of d–d transition were used to evaluate the bonding parameters α^2, β^2, and γ^2, which may be regarded as measures of the covalency of the in-plane σ bonds, in-plane π bonds, and out-of-plane π bonds.

Molecular orbital coefficients α^2 (covalent in-plane σ bonding), β^2 (covalent in-plane π bonding), and γ^2 (out-plane π bonding) were calculated using the following equations:

$$\alpha^2 = \left(A_{\|}/0.036\right) + \left(g_{\|} - 2.0027\right) + 3/7(g_{\perp} - 2.0023) + 0.04 \quad (2)$$

If the α^2 value is 0.5, it indicates complete covalent bonding, while the value of $\alpha^2 = 1.0$ suggests complete ionic bonding. The observed value of α^2 (0.72) indicates that the complex has some covalent character.

TABLE 3 Electronic Absorption Spectral Data of the Complexes in DMSO Solution

Compound	Solvent	Absorption (cm^{-1})	Band assignment	Geometry
L^1	DMSO	31,300	INCT	—
HL^2	DMSO	30,581	INCT	—
$[FeL^1L^2\ Cl_2]$	DMSO	19,064, 20,265	$^6A_{1g}\rightarrow{}^4T_{1g}(G)$ and $^6A_{1g}\rightarrow{}^4T_{1g}(G)$	Octahedral
$[CoL^1L^2]$ Cl	DMSO	18,651, 31,532	$^1A_{1g}\rightarrow{}^1B_g$ INCT	Square planar
$[NiL^1L^2]$ Cl	DMSO	20,126, 18,670	$^1A_{1g}\rightarrow{}^1B_{1g}$ and $^1A_{1g}\rightarrow{}^1B_{2g}$	Square planar
$[CuL^1L^2]$Cl	DMSO	18,302, 20,823	INCT $^2B_{1g}\rightarrow{}^2A_{1g}$	Square planar
$[ZnL^1L^2]$ Cl	DMSO	22,172	L→M	Square planar

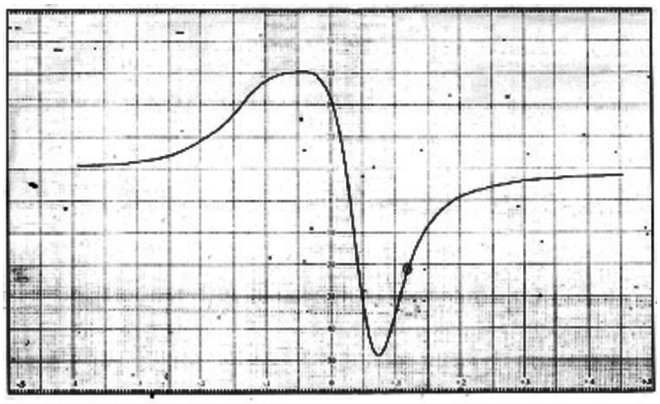

(a) (300 K)

(b) (77 K)

FIGURE 3 ESR spectrum of copper complex at room (a) and liquid temperature (b).

$$\beta^2 = \left(g_{||} - 2.0027\right)E/ - 8\lambda\alpha^2 \qquad (3)$$

$$\gamma^2 = \left(g_{||} - 2.0027\right)E/ - 2\lambda\alpha^2 \qquad (4)$$

The observed β^2 and γ^2 values of 1.23 and 0.71 indicate that there is interaction in the out-of-plane π bonding, whereas the in-plane π bonding is predominantly ionic. Significant information about the nature of bonding in the Cu(II) complex can be derived from the relative magnitudes of $K_{||}$ and $K_{\perp}$.

$$K_{||} = \alpha^2\beta^2 \qquad (5)$$

$$K_{\perp} = \alpha^2\gamma^2 \qquad (6)$$

For the present complex, the observed order $K||(0.89) > K_{\perp}(0.51)$ implies a greater contribution from out-of-plane π bonding than from in-plane π bonding in metal–ligand π bonding.

The empirical factor $f = g_{///}/A_{//}$ cm^{-1} is an index of tetragonal distortion. Values of this factor may vary from 105 to 135 for small to extreme distortions in square planar complexes, and it depends on the nature of the coordinated atoms.[20] The f values of copper complexes were found to be in the range of 144 (Table 4), indicating significant distortion from planarity.

Mass Spectra

The FAB mass spectra of the Schiff bases and their corresponding metal complexes were recorded and their stoichiometry compositions compared. The Schiff base ligands L^1 and HL^2 show a molecular ion peak at m/z = 281 and 242, respectively. The mass spectra of Fe(III), Co(II), Ni(II), Cu(II), and Zn(II) complexes show a molecular ion peak (M+) at m/z 648, 616, 617, 620, and 622 respectively, the

TABLE 4 ESR Spectral Data of the Copper Complex

Complex	$g_{||}$	$g_{\perp}$	g_{iso}	$A_{||}$	$A_{\perp}$	$K_{||}$	$K_{\perp}$	α^2	β^2	γ^2	$f = (g_{||}/A_{||})$
$[CuL^1L^2]$ Cl at 300 K	—	—	2.09	—	—	—	—	—	—	—	—
$[CuL^1L^2]$Cl at 77 K	2.21	2.02	—	153	31	0.89	0.51	0.72	1.23	0.71	144

stoichiometry of the complexes as supported by the FAB mass spectra of other complexes. Elemental analysis values are in good agreement with the values calculated from molecular formula of these complexes, which is further supported by the FAB-mass studies of representative complexes.

Solvatochromism

The complexes are soluble in various organic solvents and presented distinctive solvatochromism. The observed colors in different solvents after irradiation of the copper complex in UV light under a UV transilluminator as illustrated in Fig. 4 and λ_{max} values are presented in Table 5. The origin of the color changes are attributed to the shift in the d–d transition of the copper (II) ions as a result of solvent–solute interactions. The broad structureless absorption band is related to the transition of the electron from the lower-energy orbitals to the hole

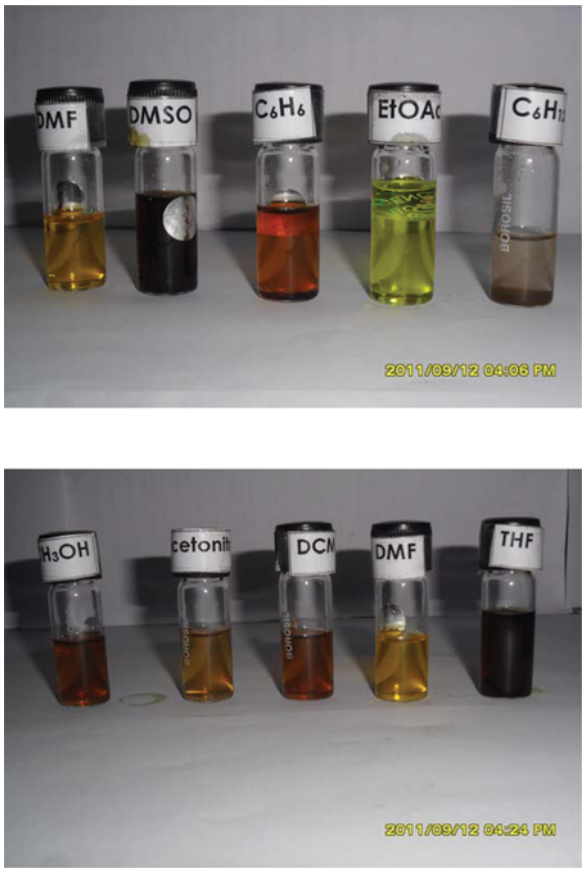

FIGURE 4 Colors in different solvents after irradiation of copper complex under UV transilluminator. (Color figure available online.)

TABLE 5 Electronic Absorption Spectral Data of Copper Complex in Various Solvents

S. No	Solvent	Wavelength, nm (λ_{max})	
		Before	After
1	DMF	682	766
2	DMSO	480	618
3	C_6H_6	657	881
4	EtOAc	450	578
5	Hexane	452	474
6	CH_3OH	459	647
7	$CH_3C \equiv N$	578	815
8	DCM	621	806
9	THF	463	718

in the $d_{x2\text{-}y2}$ orbital of the copper (II) ion (d^9). The large shifts observed for the copper complex indicate that it has larger polarizability due to the electron-withdrawing group. The obtained results suggest that the DN (donor nitrogen) parameter of solvent has the dominate contribution to the shift of the d–d absorption band of the complexes. The d–d visible absorption band exhibits a red shift with the increase of the donor number of the solvents. Similar solvatochromic behavior was observed for all other metal complexes.

DNA-Binding Studies

The ability of complexes to bind DNA was investigated by electronic absorption spectra and cyclic voltammetry.

Absorption Spectral Features of DNA Binding

The application of electronic absorption spectroscopy in DNA-binding studies is one of the most useful techniques. Complex binding with DNA through intercalation usually results in hypochromism and bathochromism, due to the intercalative mode involving a strong stacking interaction between an aromatic chromophore and the base pairs of DNA. The extent of the hypochromism commonly parallels the intercalative binding strength.[21] The absorption spectra of complexes in the absence and presence of CT-DNA of complexes are given in Fig. 5a–e.

The binding results show that the bathochromic shift of 2–4 nm along with significant hypochromicity was observed with the addition of DNA to

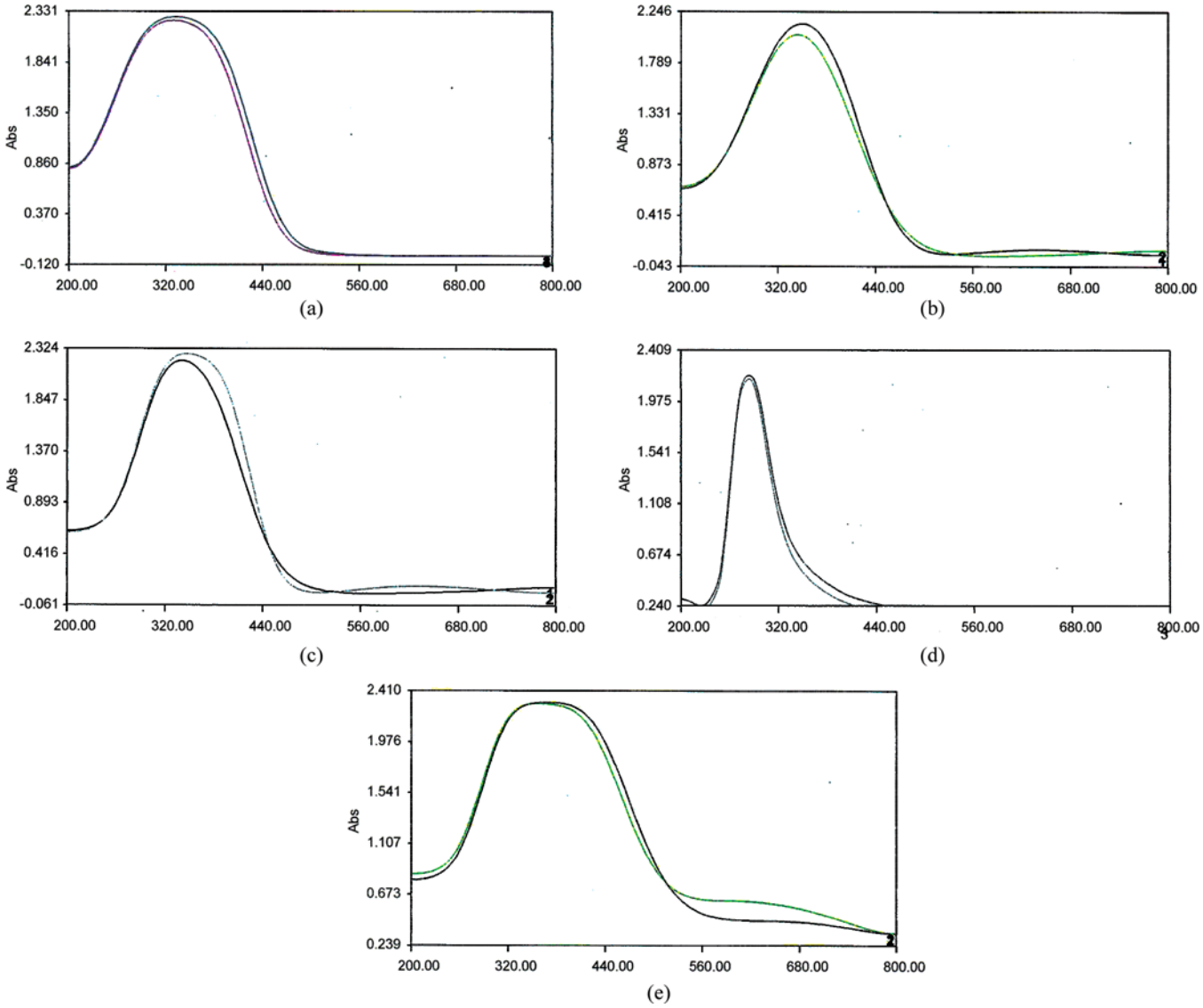

FIGURE 5 **The absorption spectra of complexes in the absence and presence of CT-DNA of complexes (a: Cu(II), b: Ni(II), c: Co(II), d: Fe(III), e: Zn(II) complexes). (Color figure available online.)**

complex solution. When the amount of CT-DNA is increased, a decrease of intensity in the charge transfer band at about 65% was observed. Intense absorption bands observed near 300 nm for complex are attributed to a $n \rightarrow \pi^*$ or $\pi \rightarrow \pi^*$ transition. To compare the binding strength of the complexes, their intrinsic binding constants (K_b) with CT-DNA have been determined from the decay of the absorbance.

The metal complexes can bind to the double-stranded DNA in different binding modes on the basis of their structure, charge, and type of ligands.[22] The observed intrinsic binding constants K_b of complexes are $4.6 \times 10^4\,M^{-1}$, $4.3 \times 10^4\,M^{-1}$, $3.9 \times 10^4\,M^{-1}$, $3.5 \times 10^4\,M^{-1}$, and $4.1 \times 10^4\,M^{-1}$, respectively. The observed K_b values of metal complexes are lower binding constants than Distamycin A.

DNA-Binding Study

In the cyclic voltammetric (CV) study, copper complexes in the presence and absence of CT-DNA are shown in Fig. 6. From CVs, it could be found that copper complexes exhibited a pair of redox peaks for one electron transfer couple of Cu(II)/Cu(I) at the scan rate of $+2$ to -2 V. The cathodic peak potential (E_{pc}) and the anodic peak potential (E_{pa}) in the absence of DNA are 0.78 and 0.26 V, respectively. The separation of the anodic and cathodic to anodic peak potentials (ΔE_p) is 206 mV, and the ratio

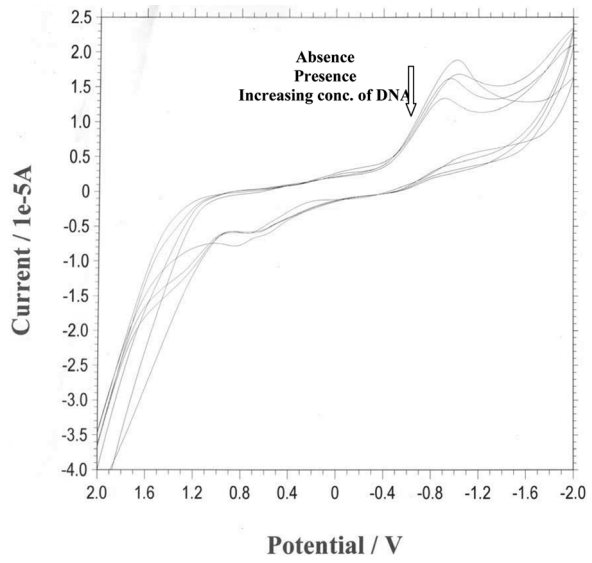

FIGURE 6 **The cyclic voltammograms of copper complexes in the absence and in the presence of various DNA concentrations.**

of cathodic to anodic peak currents i_{pc}/i_{pa} is 1.03, indicating a quasi-reversible redox process (ΔE_p of 59 mV for a one-electron diffusion and i_{pc}/i_{pa} of about one controlled reversible process). The formal potential ($E_{1/2}$), taken as the average of E_{pc} and E_{pa}, is 0.483 V in the absence of DNA. The presence of DNA in the solution at the same concentration of the copper complex causes a negative shift in E of 0.483 V and a decrease in ΔE of 0.251 V. The value of i_{pc}/i_{pa} also decreases with the increase of DNA concentration. The decrease in peak currents can be explained in terms of an equilibrium mixture of free and DNA-bound copper (II) complex to the electrode surface. These results clearly suggest that copper complex binds to CT-DNA through an intercalating way. Electrochemical parameters for the mixed ligand complexes on interaction with CT-DNA are shown in Table 6.

Superoxide Dismutase (SOD) Mimic Activities

The SOD activities of complexes were investigated by the NBT assay method. In the present study, we prepared different mixed ligand complexes. Among the metal complexes, the copper complex showed better SOD activity than other complexes. The mechanism of SOD activity is given in Eqs. (7) and (8):

$$Cu^{2+} + O_2^{-\cdot} \rightarrow Cu^{+} + O_2 \quad (7)$$

$$Cu^{+} + O_2^{-\cdot} + 2H^{+} \rightarrow Cu^{2+} + H_2O_2 \quad (8)$$

Figure 7 represents the plot of percentage of inhibiting NBT reduction with an increase in the concentration of complexes. The copper (II) complexes showed SOD-like activity, which was evaluated by the scavenger concentration causes 50% inhibition in the detector formation, IC_{50}. The observed findings indicate that the superoxide scavenging properties and oxidative behavior of mixed ligand complexes were identical to those of complexes supporting the above mechanism, which are reinforced by ESR spectral data.

Antimicrobial Activity

The in vitro biological screening effects of the investigated compounds were tested against the bacterial species and fungal species by the disc diffusion method. The MIC values of the synthesized compounds are summarized in Tables 7 and 8. A comparative study of the mixed ligands and their complexes (MIC values) indicates that complexes exhibit higher antimicrobial activity than the free ligands. The enhanced activity of the complexes can be explained on the basis of Overtone's concept[23] and Tweedy's chelation theory.[24] According to Overtone's concept of cell permeability, the lipid membrane that surrounds the cell favors

TABLE 6 **Electrochemical Parameters for the Mixed Ligand Complexes on Interaction with CT DNA**

		$E_{1/2}$(V)		△Ep(V)		
Compound	Redox couple	Free	Bound	Free	Bound	Ip_a/Ip_c
$[FeL^1L^2\ Cl_2]$	Fe (III)→Fe(II)	−0.218	−0.310	0.439	0.486	1.29
$[CoL^1L^2]$ Cl	Co(III)→Co(II)	−0.245	−0.321	0.431	0.441	1.21
$[NiL^1L^2]$ Cl	Ni(II)→Ni(I)	−0.231	−0.248	−0.431	−0.416	1.02
$[CuL^1L^2]$Cl	Cu(II)→Cu(I)	0.301	0.270	0.483	0.251	1.18
$[ZnL^1L^2]$ Cl	Zn(II)→Zn(0)	−0.347	−0.353	0.338	−0.310	0.81

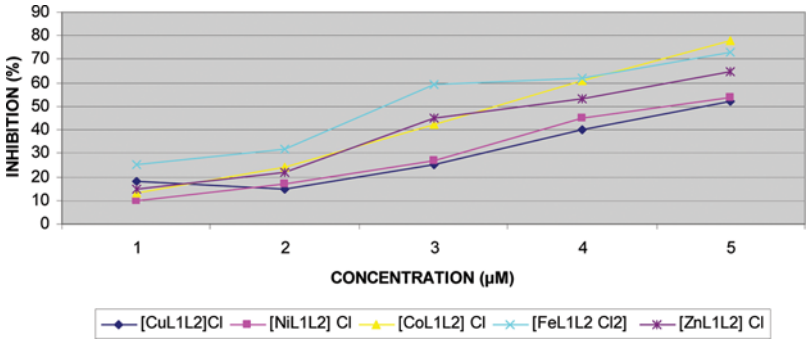

FIGURE 7 **Plot of percentage of inhibiting NBT reduction with an increase in the concentration of complexes. (Color figure available online.)**

TABLE 7 **Minimum Inhibitory Concentration of the Synthesized Compounds Against Growth of Bacteria (μg/mL)**

Compound	*E .coli*	*K. pneumonia*	*S. typhi*	*P. aeruginosa*	*S. aureus*
L^1	60	64	66	66	72
HL^2	58	62	58	59	69
$FeCl_3.6H_2O$	79	82	86	82	91
$CoCl_2.6H_2O$	81	68	72	78	89
$NiCl_2.6H2O$	66	74	81	85	83
$CuCl_2.2H_2O$	82	85	87	91	88
$ZnCl_2$	75	81	81	92	83
$[FeL^1L^2\ Cl_2]$	43	58	62	59	52
$[CoL^1L^2]$ Cl	51	55	61	63	51
$[NiL^1L^2]$ Cl	49	56	52	65	53
$[CuL^1L^2]$Cl	52	54	58	60	63
$[ZnL^1L^2]$ Cl	50	42	55	63	51
Penicillin	10	15	6	12	4
Ampicillin	12	10	8	4	6
Vancomycin	6	14	12	10	8
Ofloxacin	8	10	4	6	14

TABLE 8 **Minimum Inhibitory Concentration of the Synthesized Compounds Against Growth of Fungi (μg/mL)**

Compound	*A. niger*	*R. stolonifer*	*A. flavus*	*R. bataicola*	*C. albicans*
L^1	60	66	72	80	50
HL^2	58	65	58	69	58
$FeCl_3.6H2O$	82	82	86	78	74
$CoCl_2.6H_2O$	94	84	82	87	83
$NiCl_2.6H2O$	82	71	73	75	81
$CuCl_2.2H_2O$	91	85	84	82	83
$ZnCl_2$	78	75	81	85	86
$[FeL^1L^2\ Cl_2]$	18	24	36	27	21
$[CoL^1L^2]$ Cl	15	28	31	24	16
$[NiL^1L^2]$ Cl	23	25	32	21	25
$[CuL^1L^2]$Cl	21	37	32	45	38
$[ZnL^1L^2]$ Cl	22	26	29	33	20
Nystatin	12	15	5	15	16
Ketoconazole	14	9	15	8	15
Clotrimazole	10	6	17	14	8

the passage of only the lipid-soluble materials, which makes liposolubility an important factor, controlling the antimicrobial activity. On chelation, the polarity of the metal ion will be reduced to a greater extent due to the overlap of the ligand orbital and partial sharing of the positive charge of the metal ion with donor groups. Further, it increases the delocalization of π-electrons over the whole chelate ring and enhances the lipophilicity of the complexes.

This increased lipophilicity enhances the permeation of the complexes into lipid membranes and blocking of the metal binding sites in the enzymes of microorganisms. These complexes also disturb the respiration process of the cell and thus block the synthesis of the proteins, which restricts further growth of the organism, and as a result, microorganisms will die. The increased activity of the complexes may also be explained on the basis of their high solubility, size of the metal ion, and presence of the bulkier organic moieties. The different lipophilic behaviors of aromatic residues such as antipyrine and furfuraldehyde are involved in the biological activity mechanisms. The rise in the antimicrobial activity of mixed ligand complexes may be owing to the effect of the metal ion on the normal cell processes.[25] The comparative study of mixed ligand complexes showed higher activity than other ligand complexes.

It has been suggested that the intracellular reduction of Cu(II) to Cu(I) species may also lead to the activation of oxygen, which could be lethal for bacteria growth and lead to cell death.

CONCLUSION

New series of mixed ligand complexes of 4-aminoantipyrine derivatives were synthesized and characterized by elemental analysis, spectral (FT-IR, UV-Vis, ^{1}H-NMR, and ESR). The electrochemical behavior of metal complexes and their interaction with DNA were investigated by electrochemical techniques. The DNA-binding properties of synthetic metal complexes have been studied by electronic absorption spectra and cyclic voltammetry. All the results suggest that the complex interaction with DNA is by minor groove-binding mode. Antimicrobial activity studies show that the complexes showed better biological activity as compared to free ligand. The mixed ligand complexes showed higher binding activity due to the presence of electron-donating methyl groups in the phenolic moiety. In conclusion, the present study has shown that copper conjugation may be advantageous in designing highly effective drugs in anti-inflammatory therapy.

ACKNOWLEDGMENTS

We express our sincere thanks to the President, Noorul Islam Centre for Higher Education, Kumaracoil, for providing research facilities and financial support. We also express our sincere thanks to the Head, Department of Chemistry, Noorul Islam Centre for Higher Education, Kumaracoil, for providing valuable research support.

REFERENCES

1. Vimal Kumar, P. M.; Radhakrishnan, P. K. Cobalt(II) complexes of 4-(1-H-1,3-benzimidazole-2-yl)-1,5-dimethyl-2-phenyl-1–2-dihydro-3-H-pyrazol-3-one incorporating various anions: Synthesis, characterization and crystal structures. *Polyhedron* **2010**, *29*, 2335–2344.
2. Patel, R. N.; Gundla, V. L. N.; Patel, D. K. Synthesis, structure and properties of some copper(II) complexes containing an ONO donor Schiff base and substituted imidazole ligands. *Polyhedron* **2008**, *27*, 1054–1060.
3. Sun, Y-X.; Wei, W-X.; Hao, Q-L.; Lu, L-D.; Wang, X. Experimental and theoretical studies on 4-(2,4-dichlorobenzylideneamino)antipyrine and 4-(2,6-dichlorobenzylideneamino)antipyrine. *Spectrochim. Acta Part A Molec. Biomolec. Spectrosc.* **2009**, *73*(4), 772–781.
4. Zhanga, R.; Dub, B.; Sunb, G.; Sunb, Y. Experimental and theoretical studies on *o*-, *m*- and *p*-chlorobenzylideneaminoantipyrines. *Spectrochim. Acta Part A Molec. Biomolec. Spectrosc.* **2010**, *75*(3), 1115–1124.
5. Mosae Selvakumar, P.; Suresh, E.; Subramanian, P. S. Synthesis, spectral characterization and structural investigation on some 4-aminoantipyrine containing Schiff base Cu(II) complexes and their molecular association. *Polyhedron* **2007**, *26*(4), 749–756.
6. Rosu, T.; Negoiu, M.; Pasculescu, S.; Pahontu, E.; Poirier, D.; Gulea, A. Metal-based biologically active agents: Synthesis, characterization, antibacterial and antileukemia activity evaluation of Cu(II), V(IV) and Ni(II) complexes with antipyrine-derived compounds. *Eur. J. Med. Chem.* **2010**, *45*(2), 774–781.
7. El-Dissouky, A.; El-Sonbati, A. Effect of substituants on the structure of dioxouranium(VI) complexes of 7-carboxaldehyde-8-hydroxyquinoline and some of its Schiff bases. *Transition Metal Chem.* **1986**, *11*, 112–115.
8. Patel, M. N.; Joshi, H. N.; Patel, C. R. DNA interaction, in vitro antimicrobial and SOD-like activity of copper(II) complexes with norfloxacin and terpyridines. *J. Organometal. Chem.* **2012**, *701*, 8–16.
9. Patel, M. N.; Dosi, P. A.; Bhatt, B. S. Antibacterial, DNA interaction and superoxide dismutase activity of drug based copper(II) coordination compounds. *Polyhedron* **2010**, *29*, 3238–3245.
10. Ismail, K. Z.; El-Dissouky, A.; Shehadab, A. Z. Spectroscopic and magnetic studies on some copper(II) complexes of antipyrine Schiff base derivatives. *Polyhedron* **1997**, *16*, 2909.
11. Raman, N.; Dhaveethu Raja, J. Synthesis, structural characterization and antibacterial studies of some biosensitive mixed ligand copper(II) complexes. *J. Ind. J. Chem.* **2007**, *46A*, 1611–1614.
12. Bhirud, R. G.; Shrivastava, T. S. Synthesis, characterization and superoxide dismutase activity of some ternary copper(II) dipeptide-2, 2′-bipyridine, 1,10-phenanthroline and 2,9-dimethyl-1,10-phenanthroline complexes. *Inorg. Chim. Acta.* **1991**, *179*, 125.

13. Mohamed, G. G.; Al-Gamel, N. E. A.; Nour El-Dien, F. A. Preparation, chemical characterization of 6-(2-pyridylazo)-3-acetamidophenol and its metal complexes. *Synth. React. Inorgan. Metal Organ. Chem.* **2001**, *31*, 347–358.
14. Dutta, R. L.; Syamal, A. *Elements of Magneto Chemistry,* 2nd ed.; East-West Press: New Delhi, 1992, pp. 203–250.
15. Iskander, M. F.; Khalil, T. E.; Werner, R.; Haase, W.; Svoboda, I.; Fuess, H. Synthesis, reactivity and magnetochemical studies on copper(II) complexes derived from *N*-salicylidenearoylhydrazines. X-ray structure of [mononitrato*OO*(−1)(*N*-salicylidenatobenzoylhydrazine) *ONO*(−1)]copper(II) monohydrate. *Polyhedron* **2000**, *19*(8), 949–958.
16. Reddy, P. S.; Reddy, K. H. Transition metal complexes of benzil-α-monoxime (BMO); X-ray structure determination of Co(BMO). *Polyhedron* **2000**, *19*(14), 1687–1692.
17. Lever, A. P. B. *Inorganic Electronic Spectroscopy,* 2nd ed.; Elsevier Science: New York, 1984.
18. Temel, H.; Ilhan, S.; Sekerci, M.; Ziyadanogullari, R. Synthesis and characterization of new Cu(II), Ni(II), Co(II) and Zn(II) complexes with Schiff base. *Spectrosc. Lett.* **2002**, *35*(2), 219–228.
19. Hathaway, B. J.; Billing, D. E. The electronic properties and stereochemistry of the mono-nuclear complexes of the copper(II) ion. *Coord. Chem. Rev.* **1970**, *5*(2), 143–207.
20. Pogni, R.; Bartoo, M. C.; Diaz, A.; Basosi, R. EPR characterization of mono(thiosemicarbazones) copper(II) complexes. Note II. *J. Inorgan. Biochem.* **2000**, *79*, 333.
21. Tan, L-F.; Chao, H.; Zhou, Y-F.; Ji, L-N. Synthesis, characterization, DNA-binding and DNA-photocleavage studies of $[Ru(bpy)_2(BPIP)]^{2+}$ and $[Ru(phen)_2(BPIP)]^{2+}$ (BPIP = 2-(4′-biphenyl)imidazo[4,5-*f*][1,10] phenanthroline). *Polyhedron* **2007**, *26*, 3029–3036.
22. Ambroise, A.; Maiya, G. Ruthenium(II) complexes of 6,7-dicyanodipyridoquinoxaline: synthesis, luminescence studies, and DNA interaction. *Inorg. Chem.* **2000**, *39*, 4264–4272.
23. Belaida, S.; Landreaub, A.; Djebbara, S.; Benali-Baiticha, O.; Bouetb, G.; Boucharac, J-P. J. Synthesis, characterization and antifungal activity of a series of manganese(II) and copper(II) complexes with ligands derived from reduced *N,N′-O*-phenylenebis(salicylideneimine). *Inorg. Biochem.* **2008**, *102*(1–2), 63–69.
24. Dharamaraj, N.; Viswanathamurthi, P.; Natarajan, K. Ruthenium(II) complexes containing bidentate Schiff bases and their antifungal activity. *Transition Metal Chem.* **2001**, *26*(1–2), 105–109.
25. Raman, N.; Sobha, S.; Selvaganapathy, M. Probing the binding mode of transition metal based biologically active compounds: Validation by spectroscopic methods. *Int. J. Pharma Bio Sci.* **2012**, *3*, 258–261.